AD-A100 451 ARMY MATERIEL DEVELOPMENT AND READINESS COMMAND ADEL--ETC F/G 9/5
SIGNAL PROCESSING THEORY OF BRAGG CELLS.(U)
MAY 81 D J TORRIERI
UNCLASSIFIED CM/CCM-81-1 NL

1 OF 1
AD
A100451

END
DATE
FILMED
7-81
DTIC

(12) LEVEL II

AD A100 [illegible]

CM/CCM-81-1

May 1981

Signal Processing Theory of Bragg Cells

by Don J. Torrieri

U.S. Army Materiel Development
and Readiness Command

Countermeasures/
Counter-countermeasures Office
2800 Powder Mill Road
Adelphi, MD 20783

UNCLASSIFIED

SECURITY CLASSIFICATION OF THIS PAGE (When Data Entered)

REPORT DOCUMENTATION PAGE

READ INSTRUCTIONS BEFORE COMPLETING FORM

1. REPORT NUMBER	CM/CCM-81-1
2. GOVT ACCESSION NO.	AD-A100 457
3. RECIPIENT'S CATALOG NUMBER	
4. TITLE (and Subtitle)	Signal Processing Theory of Bragg Cells.
5. TYPE OF REPORT & PERIOD COVERED	Technical Report.
6. PERFORMING ORG. REPORT NUMBER	
7. AUTHOR(s)	Don J. Torrieri
8. CONTRACT OR GRANT NUMBER(s)	DA: 1S263749D462
9. PERFORMING ORGANIZATION NAME AND ADDRESS	Countermeasures/Counter-countermeasures Office, 2800 Powder Mill Road Adelphi, MD 20783
10. PROGRAM ELEMENT, PROJECT, TASK AREA & WORK UNIT NUMBERS	Program Ele: 6.37.49.A
11. CONTROLLING OFFICE NAME AND ADDRESS	U.S. Army Materiel Development and Readiness Command Alexandria, VA 22333
12. REPORT DATE	May 1981
13. NUMBER OF PAGES	22
14. MONITORING AGENCY NAME & ADDRESS (if different from Controlling Office)	
15. SECURITY CLASS. (of this report)	UNCLASSIFIED
15a. DECLASSIFICATION/DOWNGRADING SCHEDULE	

16. DISTRIBUTION STATEMENT (of this Report)

Approved for public release; distribution unlimited.

17. DISTRIBUTION STATEMENT (of the abstract entered in Block 20, if different from Report)

18. SUPPLEMENTARY NOTES

ERADCOM Project: N491N1
DRCMS Code: 623749.46.20011

19. KEY WORDS (Continue on reverse side if necessary and identify by block number)

Spatial-integrating correlator
Correlation, acousto-optical
Frequency estimation, acousto-optical
Fourier transformation, acousto-optical
Time-integrating correlator
Acousto-optics
Bragg cell

20. ABSTRACT (Continue on reverse side if necessary and identify by block number)

The theory of the acousto-optical interaction has been investigated in many papers. In this paper, the fundamental theory is used to develop a basic theory that explains the signal processing capabilities of Bragg cell devices. Examples of devices for frequency estimation, correlation, and Fourier transformation are presented.

DD FORM 1 JAN 73 1473 EDITION OF 1 NOV 65 IS OBSOLETE

UNCLASSIFIED

 SECURITY CLASSIFICATION OF THIS PAGE (When Data Entered)

CONTENTS

FIGURES

1. INTRODUCTION

The interaction of light and sound can be described in terms of wave interactions or particle collisions. Both pictures are intuitively appealing and can provide basic information without elaborate mathematics. In this section, a heuristic analysis is given by using an elementary particle picture. For more precise information, such as the dependence of the interaction on acoustic power, elaborate mathematics is unavoidable and is presented in the literature.[1,2]

In the particle picture, light consists of photons and sound consists of phonons. Each photon has momentum $\hbar\mathbf{K}$ and energy $\hbar\omega_{\ell}$, where $2\pi\hbar$ is Planck's constant, $\mathbf{K}$ is the wave vector, and ω_{ℓ} is the angular frequency. Each phonon has momentum $\hbar\mathbf{k}_a$ and energy $\hbar\omega_a$, where $\mathbf{k}_a$ is the wave vector and ω_a is the angular frequency. When a photon and a phonon collide, one of two results is possible: either the phonon is annihilated or a new phonon is created. The possibilities are illustrated in figure 1, where $\mathbf{K}'$ denotes the wave vector of the scattered photon. If it is assumed that, to a good approximation, the momentum is conserved in a collision, then phonon annihilation implies

$$\mathbf{K}' = \mathbf{K} + \mathbf{k}_a , \tag{1}$$

and phonon creation implies

$$\mathbf{K}' = \mathbf{K} - \mathbf{k}_a . \tag{2}$$

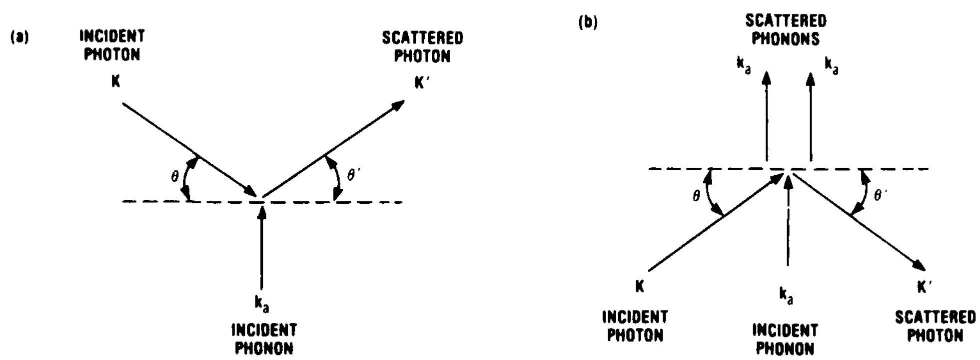

Figure 1. Photon-phonon interactions: (a) annihilation and (b) creation.

---

[1] *I. C. Chang, Acousto-Optic Devices and Applications, IEEE Trans. Sonics Ultrason.,* <u>*23*</u> *(January 1976), 2.*

[2] *M. Born and E. Wolf, Principles of Optics, 5th ed., Pergamon Press, Inc., New York (1975).*

We examine the implications of equation (1) in detail; the implications of equation (2) are analogous. From equation (1) and figure 1(a), we have

$$K' \cos \theta' = K \cos \theta , \tag{3}$$

$$K' \sin \theta' = k_a - K \sin \theta , \tag{4}$$

where K', K, and k_a are the magnitudes of the corresponding wave vectors, θ is the angle of the incident photon, and θ' is the angle of the scattered photon. If θ, k_a, and λ are specified, equations (3) and (4) can be solved for θ' and K'. Dividing equation (4) by equation (3) yields

$$\theta' = \tan^{-1} \left[- \tan \theta + \left(\frac{k_a}{K} \right) \sec \theta \right] . \tag{5}$$

Assuming that $k_a/K << 1$ and $\theta << 1$, equation (5) gives

$$\theta' \simeq \frac{k_a}{K} - \theta . \tag{6}$$

Let v and c represent the acoustic and optical velocities, respectively. Since we know from wave theory that $v = \omega_a/k_a$ and $c = \omega_\ell/K$,

$$\frac{k_a}{K} = \frac{c\omega_a}{v\omega_\ell} . \tag{7}$$

Thus,

$$\theta' \simeq \left(\frac{c}{v\omega_\ell} \right) \omega_a - \theta . \tag{8}$$

This relation shows explicitly that the angle of the scattered photon with respect to the incident direction is proportional to the acoustic frequency. Although the acousto-optical interaction may consist of multiple collisions of photons with phonons, it turns out that equation (8) does hold approximately for many practical devices. Thus, a diffracted beam is deflected at an angle proportional to the acoustic frequency. If the angle is measured, the acoustic frequency can be estimated.

We define the Bragg angle, θ_B, by

$$\sin \theta_B = \frac{k_a}{2K} . \tag{9}$$

If $\theta = \theta_B$, equation (5) implies that $\theta' = \theta = \theta_B$. Equation (3) then gives $K' = K$. Thus, the magnitude of the photon momentum is conserved when the photon is incident at the Bragg angle. It turns out that $\theta = \theta_B$ is the condition for the most efficient diffraction of an optical wave in an isotropic medium. Figure 2 is a wave vector diagram for the Bragg condition.

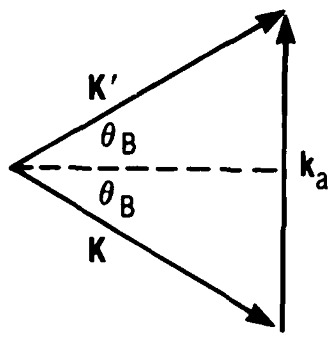

Figure 2. Wave vectors for Bragg angle of incidence.

The conservation of energy is approximately valid for a photon-phonon collision. Thus, the frequency of a scattered photon is

$$\omega_0 = \omega_\ell + \omega_a \tag{10}$$

for phonon annihilation and

$$\omega_0 = \omega_\ell - \omega_a \tag{11}$$

for phonon creation. It turns out that the frequency of the principal diffracted wave satisfies equation (10) or equation (11) in many practical devices.

Birefringent diffraction, which occurs when the refractive indices for the incident and diffracted optical waves are different, exhibits significantly different characteristics from isotropic diffraction.[1,3] In an anisotropic medium, a change in direction and polarization between the incident and diffracted waves causes birefringent diffraction. Since $\omega_a \ll \omega_\ell$, we have $\omega_0 \approx \omega_\ell$ in practical cases. Thus, $K' \approx rK$, where r is the ratio of the refractive index associated with the diffracted wave to the refractive index associated with the incident wave. We expect a large principal diffracted beam if conservation of momentum is satisfied. Using trigonometry in equations (3) and (4), we obtain the necessary conditions:

---

[1] *I. C. Chang, Acousto-Optic Devices and Applications, IEEE Trans. Sonics Ultrason.,* 23 *(January 1976), 2.*

[3] *J. Sapriel, Acousto-Optics, John Wiley & Sons, Inc., New York (1979).*

$$\sin\theta = \frac{k_a}{2K}\left[1 + \left(\frac{K}{k_a}\right)^2 \left(1 - r^2\right)\right], \tag{12}$$

$$\sin\theta' = \frac{k_a}{2Kr}\left[1 - \left(\frac{K}{k_a}\right)^2 \left(1 - r^2\right)\right]. \tag{13}$$

With these equations, we can derive several interesting results.

To observe $\theta' = \theta$, we must have $r = 1$ or $r = (k_a | K) - 1$. The latter equation cannot be satisfied since $k_a < K$. Thus, $\theta' = \theta$ is a phenomenon associated with $r = 1$ and the Bragg angle of incidence.

Equations (12) and (13) do not have solutions unless the right-hand sides have magnitudes less than or equal to unity. This requirement and $k_a < K$ yield

$$1 - \frac{k_a}{K} \leqslant r \leqslant 1 + \frac{k_a}{K}. \tag{14}$$

Thus, strong acousto-optical diffraction is usually not observed unless equation (14) is satisfied.

If we specify θ, equation (12) gives two possible values of k_a, and equation (13) gives two corresponding values of θ'. Thus, for an incident wave vector $\mathbf{K}$, there are two values of k_a that allow conservation of momentum, as illustrated in figure 3, where n_0 and n_1 are the refractive indexes for the incident and diffracted beams, respectively.

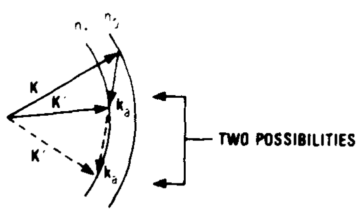

Figure 3. Possible wave vectors giving conservation of momentum.

Birefringent diffraction is important primarily because the conservation of momentum can be approximately satisfied over a wider range of acoustic frequencies or incident light directions than is usually possible with isotropic diffraction. Consequently, anisotropic materials are useful in devices requiring a large bandwidth.

2. BRAGG CELL INTERACTIONS

In this section, acousto-optical theoretical results are summarized and used to develop the basic theory needed for most applications.

An acoustic wave traveling through a crystalline medium produces a spatial variation in the density of the medium. This variation causes changes in the refractive index. When light enters the medium, it is diffracted by the spatially varying refractive index. The acoustic wave is generated from an electrical signal by a piezoelectric transducer attached to the medium. As a result of the acousto-optical interaction, the diffracted light emerging from the medium is modulated by the information contained in the original electrical signal. Since the modulated light has a spatial variation equivalent to the time variation of the signal, parallel processing of information is possible.

The diffraction geometry associated with the acousto-optical interaction is shown in figure 4, where λ_a is the acoustic wavelength. Let the angular frequency and the wave vector of the incident optical wave in the medium be denoted by ω_ℓ and $\mathbf{K}$, respectively, and those of the acoustic wave by ω_a and $\mathbf{k}_a$. Due to the acousto-optical interaction, the diffracted optical waves in the medium have angular frequencies $\omega_m = \omega_\ell + m\omega_a$ and approximate wave vectors $\mathbf{K}_m = \mathbf{K} + m\mathbf{k}_a$, where $m = \pm 1, \pm 2, \ldots$. Special cases of diffraction can be characterized by the parameter

$$Q = \frac{k_a^2 L}{K} , \tag{15}$$

where k_a and K are the magnitudes of the acoustic and optical wave vectors, respectively, and L is the width of the acoustic beam. When $Q < 1$, the diffraction is said to be in the Raman-Nath regime. When $Q >> 1$, the diffraction is said to be in the Bragg regime. The intermediate region where $1 < Q < 10$ gives a mixture of the characteristics of the Raman-Nath and Bragg regimes.

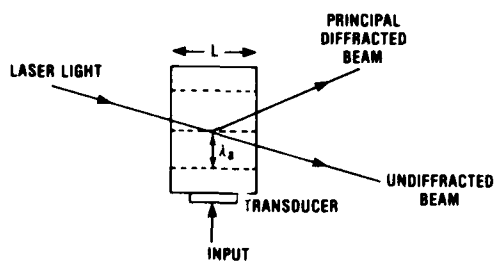

Figure 4. Bragg cell interaction.

In the Raman-Nath regime, many diffracted beams may contain significant power. This regime corresponds to ultrasonic frequencies less than 20 MHz if $L \simeq 1$ cm, the wavelength of light is approximately 0.5 μm, and the acoustic velocity is approximately $3.5 \cdot 10^5$ cm/s.

Most of the practical wide-bandwidth applications of acousto-optics depend upon operation in the Bragg regime. An acoustical device operating in the Bragg regime is called a Bragg cell. The result of the acousto-optical interaction in a Bragg cell is the production of only two significant beams outside the cell: the undiffracted main beam and the principal diffracted beam. These beams are indicated in figure 4.

Let $\hat{\mathbf{K}}$ and $\hat{\mathbf{k}}_a$ represent unit vectors in the directions of $\mathbf{K}$ and $\mathbf{k}_a$, respectively. If $\hat{\mathbf{K}} \cdot \hat{\mathbf{k}}_a < 0$, the principal diffracted beam has a wave vector $\mathbf{K} + \mathbf{k}_a$ and an angular frequency $\omega_\ell + \omega_a$. If $\hat{\mathbf{K}} \cdot \hat{\mathbf{k}}_a > 0$, the principal diffracted beam has a wave vector $\mathbf{K} - \mathbf{k}_a$ and an angular frequency $\omega_\ell - \omega_a$. For definiteness, we assume the latter case in the remainder of this section and the next two sections.

Let θ denote the acute angle between $\hat{\mathbf{K}}$ and the acoustic wave front (perpendicular to $\hat{\mathbf{k}}_a$). We have

$$\sin \theta = \hat{\mathbf{K}} \cdot \hat{\mathbf{k}}_a \; . \qquad (16)$$

In an isotropic medium, the Bragg angle, θ_B, is defined by

$$\sin \theta_B = \frac{k_a}{2K} = \frac{c\omega_a}{2nv\omega_\ell} \; , \qquad (17)$$

where n is the index of refraction, v is the acoustic velocity, and c is the free-space velocity of light. The power in the principal diffracted beam varies with θ, attaining a maximum when $\theta = \theta_B$.

We derive the basic wave vector relations for a Bragg cell. Consider a light wave incident upon a Bragg cell at angle ϕ_i, as illustrated in figure 5. According to Snell's law, the angle θ_0 satisfies

$$n \sin \theta_0 = \sin \phi_i \; . \qquad (18)$$

The refracted light has the two-dimensional wave vector

$$\mathbf{K} = K\left(\cos \theta_0, \sin \theta_0\right) \qquad (19)$$

with magnitude

$$K = \frac{n\omega_\ell}{c} \; . \qquad (20)$$

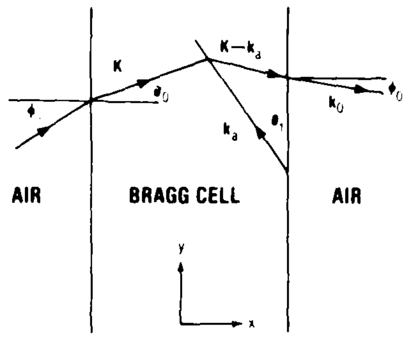

Figure 5. Diffraction geometry of Bragg cell for tilted acoustic wave.

The acoustic wave in the cell propagates at an angle θ_1 with respect to the y-axis. Thus, this tilted wave has the wave vector

$$\mathbf{k}_a = k_a(-\sin\theta_1, \cos\theta_1) \tag{21}$$

with magnitude

$$k_a = \frac{\omega_a}{v} . \tag{22}$$

After the acousto-optical interaction, the wave vector of the principal diffracted beam is $\mathbf{K}' = \mathbf{K} - \mathbf{k}_a$. Refraction as this beam leaves the cell results in a diffracted beam in air with wave vector $\mathbf{k}_0$. From electromagnetic theory, it follows that k_{0y}, the y-component of $\mathbf{k}_0$, is equal to the y-component of $\mathbf{K}'$. Thus,

$$\begin{aligned} k_{0y} &= K \sin\theta_0 - k_a \cos\theta_1 \\ &= \frac{n\omega_\ell}{c}\sin\theta_0 - \frac{\omega_a}{v}\cos\theta_1 . \end{aligned} \tag{23}$$

The x-component of $\mathbf{k}_0$ is found by observing that

$$k_0^2 = k_{0x}^2 + k_{0y}^2 = \left(\frac{\omega_\ell - \omega_a}{c}\right)^2 \tag{24}$$

since the diffracted wave has frequency $\omega_\ell - \omega_a$. The angle ϕ_0 of the diffracted beam with respect to the x-axis satisfies

$$\sin\phi_0 = \frac{k_{0y}}{k_0} . \tag{25}$$

A number of special cases are of particular interest. In general, $\omega_a << \omega_\ell$ so that $k_0 \simeq \omega_\ell/c$. Thus, equations (18) and (23) to (25) give

$$\sin \phi_0 \simeq \sin \phi_i - \frac{k_a \cos \theta_1}{k_0} . \qquad (26)$$

In general, $k_a << k_0$. If ϕ_i and θ_1 are small, we obtain

$$\phi_0 \simeq \phi_i - \left(\frac{c}{v\omega_\ell}\right) \omega_a , \quad \phi_i, \theta_1 << 1 . \qquad (27)$$

This equation establishes the fundamental relation between the acoustic frequency and the deflection of the principal diffracted beam when $\mathbf{K} \cdot \mathbf{k}_a > 0$. In figure 5, $\phi_i > 0$, $\theta_0 > 0$, and $\theta_1 > 0$, but $\phi_0 < 0$.

Another special case occurs if the angles are made to satisfy $\theta_0 = 2\theta_1$. It is convenient to define the Bragg frequency, ω_B, by

$$\omega_B = \frac{2nv\omega_\ell}{c} \sin \theta_1 . \qquad (28)$$

Equations (23) and (28) and the relation $\sin 2\theta_1 = 2 \sin \theta_1 \cos \theta_1$ yield

$$k_{0y} = \left(\frac{\omega_B - \omega_a}{v}\right) \cos \theta_1 . \qquad (29)$$

Thus, if $\omega_a = \omega_B$, the principal diffracted beam emerging from the Bragg cell is perpendicular to the cell-air interface ($\phi_0 = 0$). It follows from equations (16), (17), (19), (21), and (28) that $\theta_0 = 2\theta_1 = 2\theta_B$ and that θ, the angle between the incident light beam and the acoustic wave front, is equal to θ_B.

In the Bragg regime, the amplitude of the principal diffracted beam is approximately proportional to the amplitude of the acoustic wave if the latter has a sufficiently small amplitude. If the bandwidth of the acoustic wave is sufficiently narrow compared with its center frequency, the acoustic amplitude in the region of wave propagation can be expressed as

$$A\left(t - \frac{x}{v}\right) = A\left(t - \frac{\hat{\mathbf{k}}_a \cdot \mathbf{r}}{v}\right) ,$$

where x is the distance along the direction of the acoustic wave, $\mathbf{r}$ is the position vector, and v is the acoustic velocity corresponding to the center frequency of A(t). Let ω_0 and $\mathbf{k}_0$ denote the frequency and the wave vector of the principal diffracted beam. Neglecting the time delay due to propagation, the principal diffracted beam is approximately represented by

$$\psi(t,\mathbf{r}) = w(\mathbf{r})A\left(t - \frac{\hat{\mathbf{k}}_a \cdot \mathbf{r}}{v}\right)\cos\left(\omega_0 t - \mathbf{k}_0 \cdot \mathbf{r}\right) , \tag{30}$$

near the acoustic device output aperture. The weighting function, $w(\mathbf{r})$, is the product of factors describing aperture size, acoustic attenuation, and optical amplitude profile.

The basic theory presented in this section leads immediately to the important applications of frequency estimation, correlation, and Fourier transformation.

3. FREQUENCY ESTIMATION

The principal components of an acousto-optical spectrum analyzer[4] are shown in figure 6. According to equation (27), the principal diffracted beam is offset from the incident beam by an angle

$$\phi_1 = \phi_i - \phi_0 \simeq \left(\frac{c}{vf_\ell}\right)f_a , \tag{31}$$

where f_a and f_ℓ are the frequencies in hertz. With the Bragg cell in the front focal plane of the lens, a Fourier transform is obtained at the back focal plane at the photodetector array. The center of the diffracted beam converges to a position a distance

$$F\phi_1 \simeq \left(\frac{Fc}{vf_\ell}\right)f_a \tag{32}$$

from the center of the corresponding undiffracted beam, where F is the focal length of the lens. Thus, the frequency f_a can be estimated by measuring the relative intensities at the photodetector array elements.

---

[4] *D. L. Hecht, Spectrum Analysis Using Acousto-Optic Filters, Optical Engineering,* 16 *(September 1977), 461.*

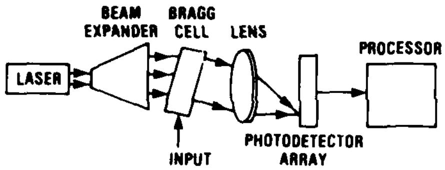

Figure 6. Acousto-optical frequency estimator.

The diffracted beam has an angular width on the order of λ_0/D, where $\lambda_0 = c/f_\ell$ is the optical wavelength in air and D is the effective aperture of the Bragg cell. Consequently, the diffracted beam spreads over a length $F\lambda_0/D$ in the focal plane. The frequency resolution is defined to be the difference in frequency between two signals such that the corresponding positions in the focal plane differ by the spread of the diffracted beam in the focal plane. From this definition and equation (32), the resolution is

$$R \simeq \frac{v}{D} = \frac{1}{T_c} , \tag{33}$$

where T_c is the time that it takes an acoustic wave to cross the cell aperture.

4. CORRELATION

The acousto-optical cross correlation of signals $A_1(t)$ and $A_2(t)$ can be accomplished by either a time-integrating correlator or a spatial-integrating correlator.[5] In the time-integrating correlator, both signals are impressed upon diffracted optical beams. Neglecting weighting functions for simplicity, we may represent the two beams by

$$\psi_1(t,\mathbf{r}) = A_1\left(t - \frac{\hat{\mathbf{k}}_{a1} \cdot \mathbf{r}}{v}\right) \cos\left(\omega_{01}t - \mathbf{k}_{01} \cdot \mathbf{r}\right) , \tag{34}$$

$$\psi_2(t,\mathbf{r}) = A_2\left(t - \frac{\hat{\mathbf{k}}_{a2} \cdot \mathbf{r}}{v}\right) \cos\left(\omega_{02}t - \mathbf{k}_{02} \cdot \mathbf{r} + \phi\right) , \tag{35}$$

[5] *R. A. Sprague, A Review of Acousto-Optic Signal Correlators, Optical Engineering,* 16 *(September 1977), 467.*

where ϕ is the phase of ψ_2 relative to ψ_1. The two beams strike an array of photodiodes. The output of a photodiode at point $\mathbf{r}$ is a time integral of the intensity of the total radiation. Thus, the output is proportional to

$$V(t,\mathbf{r}) = \int_{t-T}^{t} \left[\psi_1(t',\mathbf{r}) + \psi_2(t',\mathbf{r})\right]^2 dt' , \tag{36}$$

where T is the duration of the integration interval. Substituting equations (34) and (35) into equation (36) and using trigonometry, we obtain

$$V(t,\mathbf{r}) = V_1(t,\mathbf{r}) + V_2(t,\mathbf{r}) + V_3(t,\mathbf{r}) , \tag{37}$$

where

$$\begin{aligned} V_1(t,\mathbf{r}) = \int_{t-T}^{t} & A_1\left(t' - \frac{\hat{\mathbf{k}}_{a1} \cdot \mathbf{r}}{v}\right) A_2\left(t' - \frac{\hat{\mathbf{k}}_{a2} \cdot \mathbf{r}}{v}\right) \\ & \times \cos\left[\left(\omega_{01} - \omega_{02}\right)t' - \left(\mathbf{k}_{01} - \mathbf{k}_{02}\right) \cdot \mathbf{r} - \phi\right] dt' , \end{aligned} \tag{38}$$

$$V_2(t,\mathbf{r}) = \frac{1}{2} \int_{t-T}^{t} \left[A_1^2\left(t' - \frac{\hat{\mathbf{k}}_{a1} \cdot \mathbf{r}}{v}\right) + A_2^2\left(t' - \frac{\hat{\mathbf{k}}_{a2} \cdot \mathbf{r}}{v}\right)\right] dt' , \tag{39}$$

$$\begin{aligned} V_3(t,\mathbf{r}) = \int_{t-T}^{t} \Bigg\{ & A_1\left(t' - \frac{\hat{\mathbf{k}}_{a1} \cdot \mathbf{r}}{v}\right) A_2\left(t' - \frac{\hat{\mathbf{k}}_{a2} \cdot \mathbf{r}}{v}\right) \cos\left[\left(\omega_{01} + \omega_{02}\right)t' \right. \\ & \left. - \left(\mathbf{k}_{01} + \mathbf{k}_{02}\right) \cdot \mathbf{r} + \phi\right] + \frac{1}{2} A_1^2\left(t' - \frac{\hat{\mathbf{k}}_{a1} \cdot \mathbf{r}}{v}\right) \cos\left(2\omega_{01}t' \right. \\ & \left. - 2\mathbf{k}_{01} \cdot \mathbf{r}\right) + \frac{1}{2} A_2^2\left(t' - \frac{\hat{\mathbf{k}}_{a2} \cdot \mathbf{r}}{v}\right) \cos\left(2\omega_{02}t' \right. \\ & \left. - 2\mathbf{k}_{02} \cdot \mathbf{r} + 2\phi\right) \Bigg\} dt' . \end{aligned} \tag{40}$$

The sinusoidal factors in equation (40) are assumed to vary much more rapidly than A_1 and A_2. Thus, if T is sufficiently large and $\omega_{01} \approx \omega_{02}$, V_3 is negligible compared with V_1 and we may neglect V_3 in the subsequent analysis. V_2 is a measure of the sum of the intensities of the two waves. If these intensities are varying slowly in time, then V_2 can be suppressed by passing V through a bandpass filter. The effect on V_1 is small if the spectrum of V_1 is concentrated away from the spectrum of V_2. If the spectra of V_1 and V_2 are similar, the presence of the spatial carrier in V_1 facilitates the separation of V_1 from V_2. The separation is implemented by digital filtering of the photodiode outputs, which provide spatial samples of $V(t,\mathbf{r})$.

Alternatively, we can eliminate V_2 by using two adjacent photodiode arrays. One of the optical beams that is applied to one array is phase shifted by π radians with respect to the corresponding optical beam that is applied to the other array. The difference between the two array outputs produces

$$\begin{aligned} V(t,\mathbf{r}) &\approx V\left(t,\mathbf{r},\phi = \phi_1\right) - V\left(t,\mathbf{r},\phi = \phi_1 + \pi\right) \\ &\approx V_1\left(t,\mathbf{r},\phi = \phi_1\right) - V_1\left(t,\mathbf{r},\phi = \phi_1 + \pi\right) \\ &= 2V_1\left(t,\mathbf{r},\phi = \phi_1\right) . \end{aligned} \tag{41}$$

If $\omega_{01} = \omega_{02}$ and we change coordinates, equation (38) gives

$$V_1(t,\mathbf{r}) = E(t,q) \cos \left[\left(\mathbf{k}_{01} - \mathbf{k}_{02}\right) \cdot \mathbf{r} + \phi\right] , \tag{42}$$

$$E(t,q) = \int_{L(t)} A_1(u)A_2(u + q)\, du , \tag{43}$$

$$L(t) = \left(t - \frac{\hat{\mathbf{k}}_{a1} \cdot \mathbf{r}}{v} - T,\ t - \frac{\hat{\mathbf{k}}_{a1} \cdot \mathbf{r}}{v}\right), \tag{44}$$

$$q = \frac{\left(\hat{\mathbf{k}}_{a1} - \hat{\mathbf{k}}_{a2}\right) \cdot \mathbf{r}}{v} . \tag{45}$$

These equations indicate that $E(t,q)$ has a spatial variation that approximates the cross correlation if $\hat{\mathbf{k}}_{a1} \cdot \mathbf{r} \neq \hat{\mathbf{k}}_{a2} \cdot \mathbf{r}$ and T is on the order of the larger of the periods of $A_1(t)$ and $A_2(t)$. The spatial frequency, $\mathbf{k}_{01} - \mathbf{k}_{02}$, in equation (42) is related to the acoustic frequencies in the Bragg cells that generate ψ_1 and ψ_2. Thus, if the spatial frequency is measured, we can sometimes obtain an estimate of an unknown acoustic frequency.

As an example, figure 7 displays one implementation of a time-integrating correlator. Light beam 1 interacts with a tilted acoustic wave generated by $A_1(t)$ to produce the diffracted beam ψ_1. The diffracted beam ψ_2 is produced analogously. If the acoustic wave vectors are given by

$$\hat{\mathbf{k}}_{a1} = \left(- \sin \theta_1, \cos \theta_1\right) ,$$
$$\hat{\mathbf{k}}_{a2} = \left(- \sin \theta_1, - \cos \theta_1\right) , \tag{46}$$

then we use

$$\hat{\mathbf{k}}_{a1} - \hat{\mathbf{k}}_{a2} = \left(0, 2 \cos \theta_1\right) , \tag{47}$$

in equations (43) and (45).

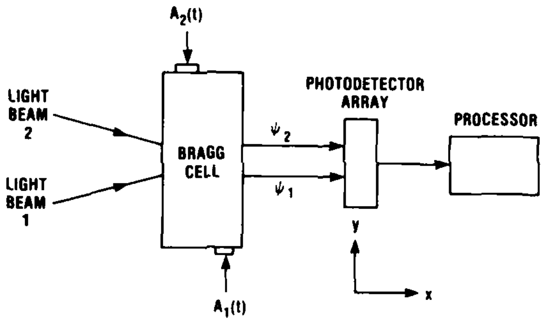

Figure 7. Time-integrating correlator.

In a spatial-integrating correlator, a beam represented by equation (34) interacts with an acoustic wave to produce a principal diffracted beam represented by

$$\psi(t,\mathbf{r}) = A_1\left(t - \frac{\hat{\mathbf{k}}_{a1} \cdot \mathbf{r}}{v}\right)A_2\left(t - \frac{\hat{\mathbf{k}}_{a2} \cdot \mathbf{r}}{v}\right) \cos \left(\omega_0 t - \mathbf{k}_0 \cdot \mathbf{r}\right) , \tag{48}$$

where $\omega_0 = \omega_{01} - \omega_{a2}$ and $\mathbf{k}_0 = \mathbf{k}_{01} - \mathbf{k}_{a2}$. For noncoherent detection, a Fourier-transforming lens is placed perpendicular to $\mathbf{k}_0$. At the center of the focal plane, the intensity is proportional to[6]

[6] *J. Goodman, Introduction to Fourier Optics, McGraw-Hill Book Co., New York (1968).*

$$I(t) = \left| \iint_R A_1\left(t - \frac{\hat{k}_{a1} \cdot r}{v}\right) A_2\left(t - \frac{\hat{k}_{a2} \cdot r}{v}\right) d^2r \right|^2 , \qquad (49)$$

where the region of integration, R, is determined primarily by the pupil of the lens and the dimensions of the acoustic devices. To simplify equation (49), we assume that the two acoustic wave vectors are oppositely directed and parallel to the y-direction, as depicted in figure 8. To within a proportionality factor, we obtain

$$I(t) = \left| \int_0^D A_1\left(t - \frac{y}{v}\right) A_2\left(t + \frac{y}{v}\right) dy \right|^2 , \qquad (50)$$

where D is the effective length of the Bragg cell. We change coordinates, drop a constant, and use $T_c = D/v$ to obtain

$$I(t) = \left| \int_{t-T_c}^{t} A_1(u) A_2(2t - u)\, du \right|^2 . \qquad (51)$$

If $A_2(t)$ is a time-reversed version of another signal $A_0(t)$, that is, if $A_2(t) = A_0(-t)$, then

$$I(t) = \left| \int_{t-T_c}^{t} A_1(u) A_0(u - 2t)\, du \right|^2 . \qquad (52)$$

This equation indicates that, for large enough T_c, the intensity at the center of the focal plane is proportional to the squared cross correlation of $A_1(t)$ and $A_0(t)$. If a photodetector is placed at the center point, its output is the squared cross correlation as a function of time.

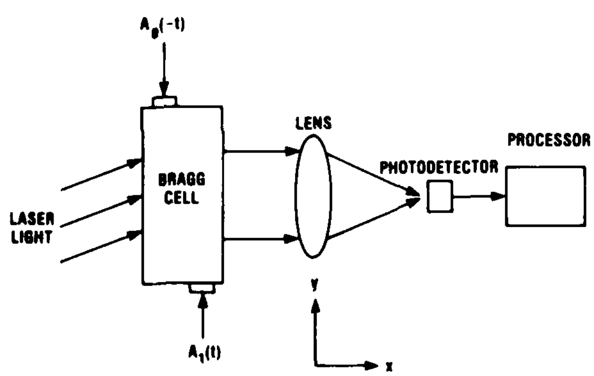

Figure 8. Spatial-integrating correlator.

A closely related technique for achieving cross correlation is to use a reference mask in place of one of the acoustic signals. Implementation details of some spatial-integrating correlators are presented by Sprague.[5]

5. FOURIER TRANSFORMATION

Acousto-optical Fourier transformation can be accomplished in a number of ways, including the use of the time-integrating correlator. Let A(t) denote the signal to be transformed. We assume that $A_1(t)$ is formed as the product of A(t) and a periodic scanning waveform. Over one scan of the waveform,

$$A_1(t) = 2A(t) \cos\left(\omega_c t + \pi\mu t^2\right) , \quad 0 \le t \le T_s , \tag{53}$$

where ω_c is the scanning frequency at t = 0, μ is the rate of frequency change, and T_s is the scan period. Let $A_2(t)$ be the scanning waveform. Thus,

$$A_2(t) = \cos\left(\omega_c t + \pi\mu t^2\right) , \quad 0 \le t \le T_s . \tag{54}$$

Substituting equations (53) and (54) into equation (43), using trigonometry, and dropping a negligible integral, we obtain the output of a time-integrating correlator due to one scan:

$$E(t,q) = \int_{L_1(t)} A(u) \cos\left(\omega_c q + 2\pi\mu qu + \pi\mu q^2\right) du , \tag{55}$$

$$L_1(t) = L(t) \cap \left[0,T_s\right] . \tag{56}$$

We may rewrite equation (55) in the form

$$E(t,q) = \mathrm{Re}\left[F(2\pi\mu q) \exp\left(j\omega_c q + j\pi\mu q^2\right)\right] , \tag{57}$$

where Re(x) denotes the real part of x, $j = \sqrt{-1}$, and

$$F(2\pi\mu q) = \int_{L(t)} A(u) \exp\left[ju(2\pi\mu q)\right] du \tag{58}$$

is an approximation of the Fourier transform at an angular frequency equal to $2\pi\mu q$. Let $|F|$ denote the magnitude and χ the phase of F. From equation (57), we obtain

---

[5] *R. A. Sprague, A Review of Acousto-Optic Signal Correlators, Optical Engineering,* 16 *(September 1977), 467.*

$$E(t,q) = |F(2\pi\mu q)| \cos\left[\omega_c q + \pi\mu q^2 + \chi(2\pi\mu q)\right] . \qquad (59)$$

Thus, the magnitude and the phase of the Fourier transform of A(u) can be approximately produced by digital processing of the photodetector array outputs.

LITERATURE CITED

(1) I. C. Chang, Acousto-Optic Devices and Applications, IEEE Trans. Sonics Ultrason., 23 (January 1976), 2.

(2) M. Born and E. Wolf, Principles of Optics, 5th ed., Pergamon Press, Inc., New York (1975).

(3) J. Sapriel, Acousto-Optics, John Wiley & Sons, Inc., New York (1979).

(4) D. L. Hecht, Spectrum Analysis Using Acousto-Optic Filters, Optical Engineering, 16 (September 1977), 461.

(5) R. A. Sprague, A Review of Acousto-Optic Signal Correlators, Optical Engineering, 16 (September 1977), 467.

(6) J. Goodman, Introduction to Fourier Optics, McGraw-Hill Book Co., New York (1968).

DISTRIBUTION

ADMINISTRATOR
DEFENSE TECHNICAL INFORMATION CENTER
ATTN DTIC-DDA (12 COPIES)
CAMERON STATION, BUILDING 5
ALEXANDRIA, VA 22314

COMMANDER
US ARMY MISSILE & MUNITIONS CENTER
AND SCHOOL
ATTN ATSK-CTD-F
REDSTONE ARSENAL, AL 35809

DIRECTOR
US ARMY MATERIEL SYSTEMS ANALYSIS
ACTIVITY
ATTN DRXSY-MP
ATTN DRXSY-CT
ABERDEEN PROVING GROUND, MD 21005

DIRECTOR
DEFENSE ADVANCED RESEARCH PROJECTS
AGENCY
TACTICAL TECHNOLOGY OFFICE
ARCHITECT BUILDING
1400 WILSON BLVD
ARLINGTON, VA 22209

DIRECTOR
DEFENSE COMMUNICATIONS ENGINEERING
CENTER
ATTN R&D OFFICE, ASST DIR FOR TECH
1860 WIEHLE AVE
RESTON, VA 22090

DIRECTOR OF DEFENSE
RESEARCH & ENGINEERING
ATTN DEP DIR (TACTICAL
WARFARE PROGRAM)
WASHINGTON, DC 20301

ASSISTANT SECRETARY OF THE ARMY
(RES, DEV, & ACQ)
ATTN DEP FOR COMM & TARGET ACQ
ATTN DEP FOR AIR & MISSILE DEFENSE
WASHINGTON, DC 20310

COMMANDER
US ARMY COMMUNICATIONS-ELEC. COMMAND
ATTN STEEP-MT-M
FORT HUACHUCA, AZ 85613

OFFICE, DEPUTY CHIEF OF STAFF FOR
OPERATIONS & PLANS
DEPARMENT OF THE ARMY
ATTN DAMO-TCD, ELECTRONIC/WARFARE
SIGNAL SECURITY
WASHINGTON, DC 20310

COMMANDER
US ARMY CONCEPTS ANALYSIS AGENCY
8120 WOODMONT AVENUE
ATTN MDCA-SMS
BETHESDA, MD 20014

COMMANDER
US ARMY COMMUNICATIONS R&D COMMAND
ATTN DRSEL-CE, COMMUNICATIONS-ELECTRONIC
SYS INTEG OFFICE
FORT MONMOUTH, NJ 07703

DIRECTOR, ELECTRONIC WARFARE LABORATORY
ATTN DELEW-V
ATTN DELEW-C
ATTN DELEW-E
ATTN DELEW-M-ST
FORT MONMOUTH, NJ 07703

COMMANDER
ELECTRONICS WARFARE LABORATORY
OFFICE OF MISSILE ELECTRONIC WARFARE
WHITE SANDS MISSILE RANGE, NM 88002

COMMANDER
NAVAL WEAPONS CENTER
ATTN CODE 35, ELECTRONIC WARFARE DEPT
CHINA LAKE, CA 93555

DIRECTOR
NAVAL RESEARCH LABORATORY
ATTN CODE 5700, TACTICAL ELE
WARFARE DIVISION
WASHINGTON, DC 20375

COMMANDER
NAVAL SURFACE WEAPONS CENTER
ATTN DF-20, ELECTRONICS WARFARE DIV
ATTN DK, WARFARE ANALYSIS DEPT
DAHLGREN, VA 22448

DIRECTOR
AF AVIONICS LABORATORY
ATTN KL (WR), ELECTRONIC WARFARE DIV
WRIGHT-PATTERSON AFB, OH 45433

COMMANDER
HQ, TACTICAL AIR COMMAND
ATTN DOR, DIR OF ELECTRONIC
WARFARE OPNS
LANGLEY AFB, VA 23665

COMMANDER
HQ USAF TACTICAL AIR WARFARE
CENTER (TAC)
ATTN ER, DCS/ELECTRONIC WARFARE
AND RECONNAISSANCE
ATTN ERW, DIR OF ELECTRONIC
WARFARE
EGLIN AFB, FL 32542

US ARMY ELECTRONICS RESEARCH &
DEVELOPMENT COMMAND
ATTN TECHNICAL DIRECTOR, DRDEL-CT
ATTN DRDEL-CCM
ATTN DRDEL-ST
ATTN DRDEL-OP
ATTN TORRIERI, D., DRDEL-CCM (20 COPIES)
ATTN LEGAL OFFICE
ADELPHI, MD 20783

INSTITUTE FOR DEFENSE ANALYSIS
400 ARMY NAVY DRIVE
ARLINGTON, VA 22209

DIA
DEP DIR OF SCIENTIFIC AND TECH INST
ELECTRONICS WARFARE BRANCH
1735 N. LYNN STREET
ARLINGTON, VA 22209

DEPT OF NAVY
OFFICE OF RES, DEV, TEST & EVAL
ATTN TACTICAL AIR SURFACE & EW DEV DIV
(NOP-98E5)
ATTN C&C EW AND SENSORS SEC
(NOP-982F3)
THE PENTAGON
WASHINGTON, DC 20350

COMMANDER
US ARMY TRAINING & DOCTRINE COMMAND
ATTN ATDC (DCS, COMBAT DEVELOPMENTS)
FT MONROE, VA 23651

OFFICE OF THE DEPUTY CHIEF OF STAFF
FOR RES, DEV, & ACQ
DEPARTMENT OF THE ARMY
ATTN DAMA-WS
ATTN DAMA-CS
ATTN DAMA-AR
ATTN DAMA-SCS, ELECTRONIC WARFARE TEAM
WASHINGTON, DC 20310

US ARMY COMBINED ARMS COMBAT DEV ACTIVITY
ATTN ATZLCA-CA
ATTN ATZLCA-CO
ATTN ATZLCA-FS
ATTN ATZLCA-SW
ATTN ATZLCA-COM-G
FT LEAVENWORTH, KS 66027

DIRECTOR
ELECTRONICS TECHNOLOGY & DEV LAB
ATTN DELET
FT MONMOUTH, NJ 07703

COMMANDER
US ARMY MATERIEL DEV & READINESS COMMAND
ATTN DRCPP
ATTN DRCPS
ATTN DRCDE
ATTN DECDE-D
ATTN DRDMD-ST
5001 EISENHOWER AVENUE
ALEXANDRIA, VA 22333

DIRECTOR
US ARMY NIGHT VISION AND ELECTRO-OPTICS
LABORATORY
FT BELVOIR, VA 22060

COMMANDER/DIRECTOR
COMBAT SURVEILLANCE AND TARGET
ACQUISITION LAB
US ARMY ERADCOM
FT MONMOUTH, NJ 07703

DIRECTOR
US ARMY SIGNLS WARFARE LAB
VINT HILL FARMS STATION
WARRENTON, VA 22186

COMMANDER
US ARMY INTELLIGENCE AND SECURITY COMMAND
ARLINGTON HALL STATION
ATTN IARDA (DCS, RDA)
ATTN IAITA (DIR, THREAT ANALYSIS)
4000 ARLINGTON BLVD
ARLINGTON, VA 22212

US ARMY TRADOC SYSTEMS ANALYSIS
ACTIVITY
ATTN ATAA-TDB
WHITE SANDS MISSILE RANGE, NM, 88002

DIRECTOR
NATIONAL SECURITY AGENCY
ATTN S65
FT MEADE, MD 20755

HARRY DIAMOND LABORATORIES
ATTN CO/TD/TSO/DIVISION DIRECTORS
ATTN RECORD COPY, 81200
ATTN HDL LIBRARY, 81100 (3 COPIES)
ATTN HDL LIBRARY, 81100 (WRF)
ATTN TECHNICAL REPORTS BRANCH, 81300
ATTN LANHAM, C., 00213
ATTN SANN, K. H., 15000 (2 COPIES)
ATTN CUNEO, J., 11400
ATTN GAYLORD, P., 11400
ATTN FLANICK, B., 11400
ATTN SHARE, S., 22100